EFDA–JET–CP(12)05/09

C. Gil, A. Barbuti, A. Boboc, S. Dorling, T. Edlington, P. Pastor, P. Spuig,
D. Simpson, B. Vincent and JET EFDA contributors

Upgrade of the Electronics of the JET Far Infrared Interferometer

Upgrade of the Electronics of the JET Far Infrared Interferometer

C. Gil[1], A. Barbuti[1], A. Boboc[2], S. Dorling[2], T. Edlington[2], P. Pastor[1], P. Spuig[1], D. Simpson[2], B. Vincent[1] and JET EFDA contributors*

JET-EFDA, Culham Science Centre, OX14 3DB, Abingdon, UK

[1]CEA, IRFM, F-13108 St-Paul-Lez-Durance, France.
[2]EURATOM-CCFE Fusion Association, Culham Science Centre, OX14 3DB, Abingdon, OXON, UK
** See annex of F. Romanelli et al, "Overview of JET Results",*
(23rd IAEA Fusion Energy Conference, Daejon, Republic of Korea (2010)).

Preprint of Paper to be submitted for publication in Proceedings of the
27th Symposium on Fusion Technology (SOFT), Liege, Belgium
24th September 2012 - 28th September 2012

ABSTRACT

For the new bicolor vertical channels of the JET Far Infrared interferometer, CEA developed analogue and digital electronics to measure by time delay counting the variation of phase of the two wavelength beams that have crossed the plasma. Algorithms to simultaneously correct, at the time scale of the period of the sine signals, the possible fringe jumps of the two wavelength signals are embedded in a FPGA processor.

Laboratory tests to validate the fringe jump corrections are reported and the first results of the phase measurements on plasmas are analyzed and compared with the data that are produced by the existing JET electronics.

1. INTRODUCTION

On JET, the integrated electron line density is obtained by measuring the phase variations of a 195 micron wavelength probe beam that crosses the plasma, compared to an external reference beam. To measure the phase, interference is created between the probe beam and another external beam that has previously been frequency shifted with 100 kHz by a rotating grating.

To reach the needed spatial resolution for local density profile determination, four vertical traversing chords are complemented by four horizontal chords that use inner vessel mirrors [1]. As these mirrors move during plasma, a second 119 micron wavelength beam is superposed on the first one to eliminate the effect of the change of the length path δ. As the two wavelength beams arrive on a single detector, the frequency shifts of the second wavelength are set differently, in order to electronically separate the two sine signals by filtering.

The measured phase ϕ can be expressed in fringe:

$$\Phi = C\lambda\int n_e \, dz + \frac{\delta}{\lambda} + F \qquad (1)$$

Where C is a constant, λ the wavelength, n_e the local density, δ the length path and F an integer that is generated by incorrect counting of the phase, also called a fringe jump.

The range of the instrument is as large as hundreds of fringes because on JET the line density can reach more than 10^{21} m^{-2}. Thus the measurement has to be continuous all through the pulse, not to be lost in the phase evaluation. Therefore, when the beam amplitude diminishes because of refraction effects for instance, corrections using the hypothesis of density stability are applied with limited success to evaluate the non physical fringe jumps F.

Recently a second laser system at a shorter wavelength of 119µm with a beat-signal frequency of 23kHz has been installed in order to get a second independent phase measurement from the vertical channels [2]. This will allow more sophisticated correction algorithms that will be able to cope with amplitude variations.

For simultaneously measuring the two phases of each vertical channel beam, a new analogue-digital electronics has been developed by CEA, benefiting from its experience on the Tore Supra tokamak interferometer electronics.

2. ANALOGUE AND DIGITAL ELECTRONICS

Figure 1 shows the global set up of the electronics for one channel. Simultaneously for the two frequencies, the analogue board TSE184 first separates the two mixed signals by a notch filter, then by a 4^{th} order band pass filter. Its width is proportional to the wavelength λ multiplied by the maximum of the expected variation speed of the line density during plasma.

After filtering, the amplitudes of the signals are adjusted to be above 2.5 volts before each pulse by a programmable amplifier tuned by an external computer: The RMS values are sent to it and the information on the needed gains is sent back to the board that applies the gain via a FPGA processor. Since the amplitude of the signals could widely vary from pulse to pulse because of unpredictable changes of laser power, the amplifier gain range has been designed to be tuned between 6dB to 36dB for the 100kHz signal and between 6dB to 52dB for the 23kHz one.

After being amplified, the sine signals are transformed into rectangular ones, in which rising edges are created at each zero-crossing detection. To be considered, the sine signals must first cross a positive threshold (0,4V) and then the zero before a pre-defined time (1.6μs for the 100kHz and 6μs for the 23kHz). This zero-crossing detection allows a better precision than the conventional hysteresis comparators and removes glitches.

The square signals are then transmitted by optical fiber to the digital TSE188 board. In the same way, the reference square signals are created in a second TSE184 and then dispatched to all the digital TSE188 boards.

In the TSE188, the phase is calculated in a FPGA processor using the VHDL language. The method to calculate the phase by the time delay between two edges has been established on the Tore Supra interferometer [3] and then tested at JET [4].

The phase Φ is calculated as:

$$\Phi = K - J + \frac{N_i}{N_K} \qquad (2)$$

Where K and J are the counting of the reference edges and probe edges, N_K and N_J are the 25 MHz counting between two edges, which correspond to the instantaneous period of the sine signals, and N_i the counting between the reference and the following in time probe edges. The phase measure is refreshed at each J edge.

The results of the calculation are then sent via Ethernet to the JET data base. The sampling rate (ms) and duration of acquisition is set in the TSE188 by a soft core processor (Altera Nios) using information sent via Ethernet by an external computer.

3. FRINGE JUMP CORRECTIONS

3.1 DETECTION OF THE ANOMALIES IN THE PHASE

When fringe jumps occur, it is better to detect them on the time scale of the period of the sine signals (resp. 10µs and 43µs) and correct them by the VHDL program.

The principle is that an anomaly is detected when the N_K or N_J counting between two edges, which normally are equal to 250 for the 100kHz signal (resp. 1087 for the 23kHz one), are outside

an interval of plausibility of [200 312]. This interval corresponds to the 80-120kHz (resp. 11-35kHz for the 23kHz) filter of the TSE184 board.

The first cause of an anomaly is a decrease of the amplitude to below the threshold that inhibits the generation of an edge in the TSE184. During plasma, one can also observe, as shown in figure 2 using a 1MHz data acquisition, large variations of the N_J (middle fig) while the amplitude (top fig) decreases but remains above the threshold.

These N_J oscillations may be the signature of a spurious signal that is superposed on the physical 100kHz one.

On can see (bottom fig 2) that the raw counting is lost and generates a density decrease. The real time JET old measurement is lost as well. In the contrary, when the anomaly is detected, the correcting algorithm keeps the density constant, which is more physical since there is no special plasma event during this time.

3.2 ALGORITHMS OF FRINGE JUMP CORRECTION

Two kinds of correction have been studied in details in ref [4] and are applied in the TSE188 board. The first corrective algorithm uses the signal of single wavelength and considers that the density has not changed during the anomaly. Figure 2 bottom is an example of this algorithm. As soon as the anomaly is detected, the counting of the phase is blocked. Then, 1ms after the recovering of the signal above the threshold, the phase is reset to the closest value of the phase that was measured 500µs before the anomaly.

The second corrective algorithm uses the phase information of the other wavelength sine signal if it has not itself been disturbed. This kind of correction is compatible with possible variations of density during the loss of the sine signal. The hypothesis is that the time length of the anomaly is short enough so that the phase change is only due to density variation and thus proportional to the wavelength. Like the first algorithm, the phase is blocked for at least 1 ms after the anomaly detection and the calculation of the phase variation is carried out by using a reference value that has been memorized 500µs before the vanishing of the beam.

3.3 VALIDATION OF THE ALGORITHMS

The two correcting algorithms have been tested in the TSE188 board using generator induced rectangular inputs by artificially suppressing in the VHDL code some of the K and J edges of the probe signal.

Figure 3 validates the first algorithm that corrects the fringe jumps when the density is constant, which is equivalent to put the same frequency on the reference and probe inputs. One can see that the corrected phase remains constant while the raw counting varies with the losses of the edges. The algorithm also detects the rate of fringe jumps in real time (bottom figure), which will be very helpful information when the phase measurement is used for machine protection.

To validate the second algorithm (figure 4) with generators, two different phase ramps down that are proportional to the wavelength have been created by a frequency discrepancy between the

reference and the probe input. Even though the signal of one frequency has disappeared, one can see that the phase corrected by the second algorithm remains on the same slope while the raw counting and first algorithm phase generate fringe jumps.

4. RESULTS WITH PLASMA

4.1 TWO WAVELENGTH COMPATIBILITY

The electronics has been tested on plasma during the 2012 JET plasma campaign that tested the ITER like wall. When no fringe jumps occur, there is a good agreement between the 100kHz real time old and new phase measurements and the 23kHz phase as well , as seen for instance in figure 5. The observed noise on the 23kHz is greater because the shorter wavelength phase measurement is more sensitive to noise and because the alignment of the beam could not be optimized during this campaign.

4.2 Analysis of the fringe jump corrections

A statistical analysis of the fringe jump efficiency of fringe jump corrections has been performed using data base from the 2012 JET campaign. Because the second wavelength was not often available, only the first algorithm using one wavelength is discussed.

Figure 6 is an example of fringe jump correction by the new electronics, when the original system fails to follow the phase history.

A good criterion to determine the efficiency of the fringe corrections is the final value of the phase after plasma. The closer to zero, the more efficient is the correction.

Figure 7 is a comparison of the integrated histograms of the number of pulses where the final phase after plasma is less than a defined value. Only the pulses without disruption have been kept for the statistics because the disruptions induce strong changes of density that the first correction algorithm cannot cope with. The efficiency of the fringe jump correction by the new electronics is globally better. Nevertheless, simulations with the 1MHz data acquisition showed some cases of over corrections, which suggests that the algorithm could be further optimized.

CONCLUSIONS

New analogue-digital electronics has been designed for the bicolor JET Far infrared interferometer and implemented with success in the JET environment.

The principle of phase measurement by time delay counting has been validated for the two wavelengths.

The real time algorithms of fringe jump corrections that are embedded in the FPGA processor, using one and two wavelengths, have been validated in laboratory.

For correcting fringe jumps that occur during plasma, the one wavelength algorithm has proven to be already more efficient than the older JET one.

Work is in progress to understand the physics behind the faulty corrections and thus improve the algorithms.

ACKNOWLEDGMENTS

This work, supported by the European Communities under the contract of Association between EURATOM and CEA, was carried out for the JET EP2 Real Time Measurement and Control Diagnostics and Infrastructure project under the framework of the European Fusion Development Agreement. The views and opinions expressed herein do not necessarily reflect those of the European Commission.

REFERENCES

[1]. Braithwaite G. et al, Review of Scientific Instruments **60**, 2825 (1989).

[2]. Boboc A. et al, Review of Scientific Instruments **83**, 10E341 (2012)

[3]. Gil C. et al, Review of Scientific Instruments, **79**, 10E710 (2008)

[4]. Gil C. et al, Review of Scientific Instruments, **81**, 10D536(2010)

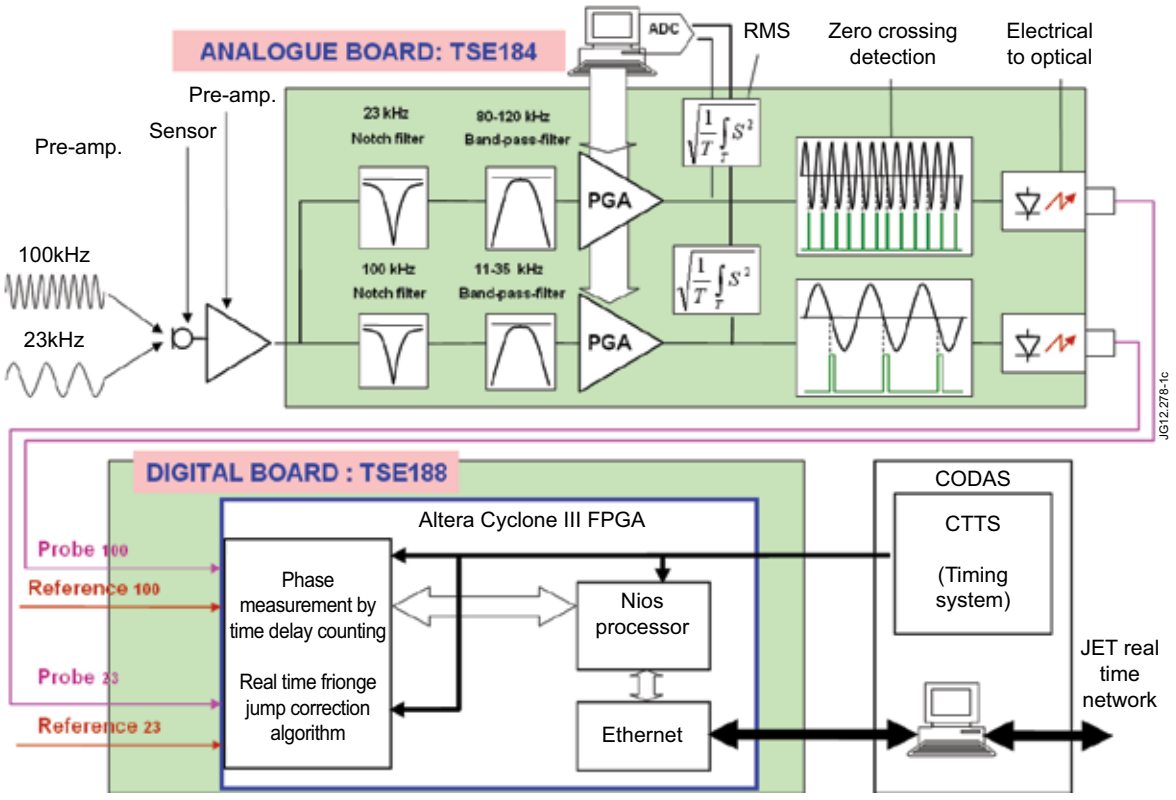

Figure 1: Electronics set up for one channel.

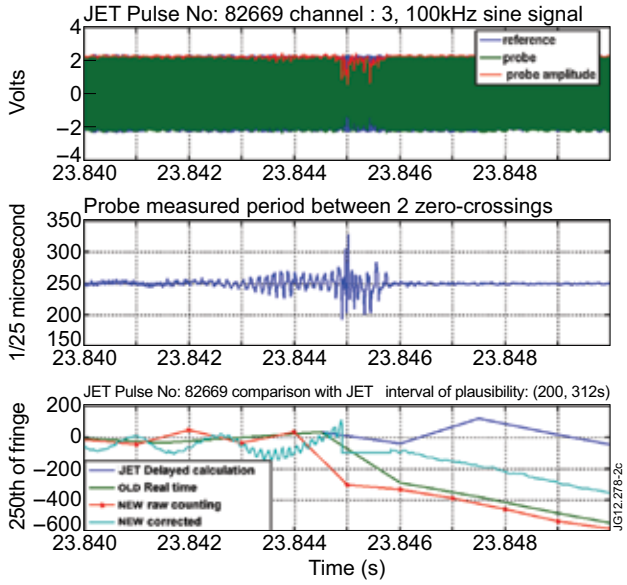

Figure 2: Top: Temporal evolution of the sine 100kHz signals during a pulse, middle: Instantaneous frequency, bottom: Calculated phase.

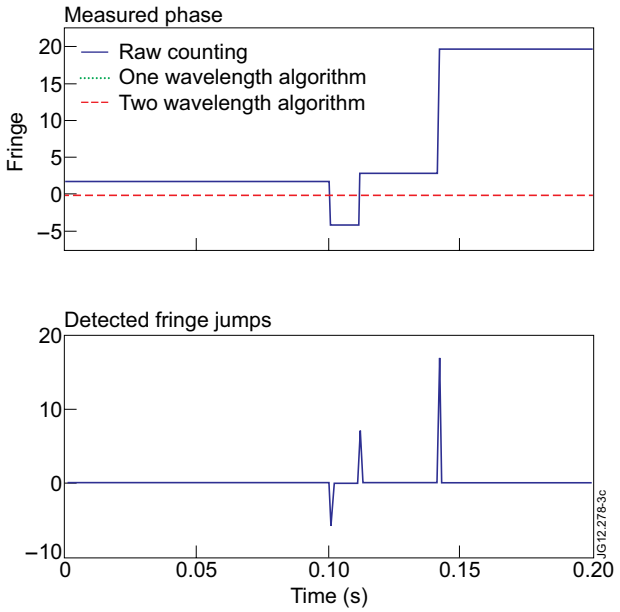

Figure 3 Validatin of the fringe jump correction with a single signal, f_{K100}=100kHz , f_{J100}=100kHz , top: Measured phase, bottom: Detected fringe jumps per millisecond.

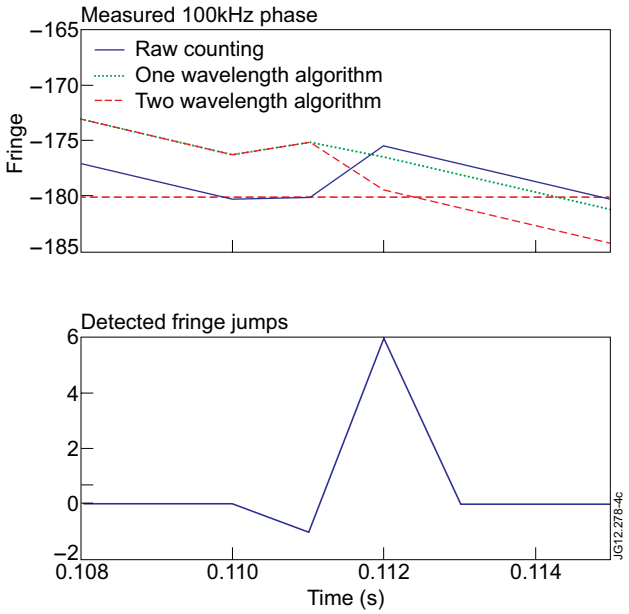

Figure 4: Validation of the fringe jump correction using the two signals, f_{K100} = 100kHz, f_{J100} = 101.6kHz, f_{K23} = 23kHz, f_{J23} = 23.98kHz, top: Measured phase, bottom: Detected fringe jumps per millisecond.

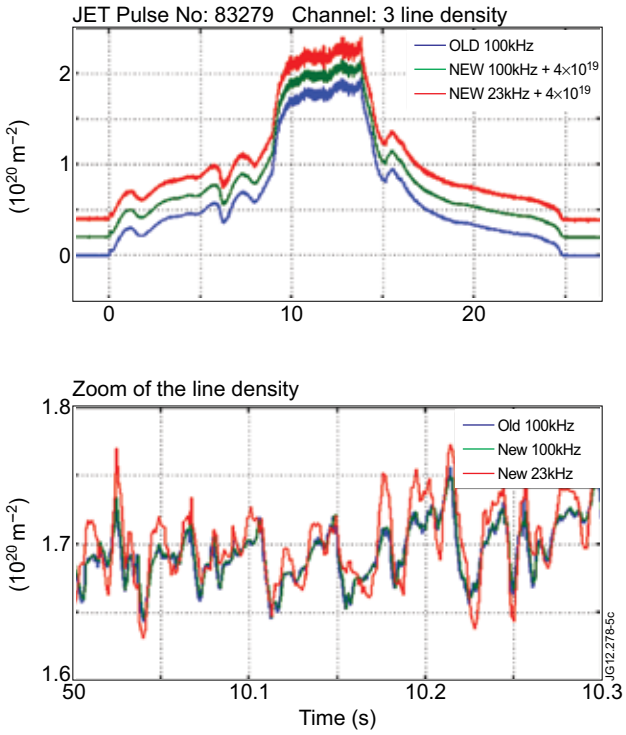

Figure 5: Comparison of the measured phase evolution during plasma.

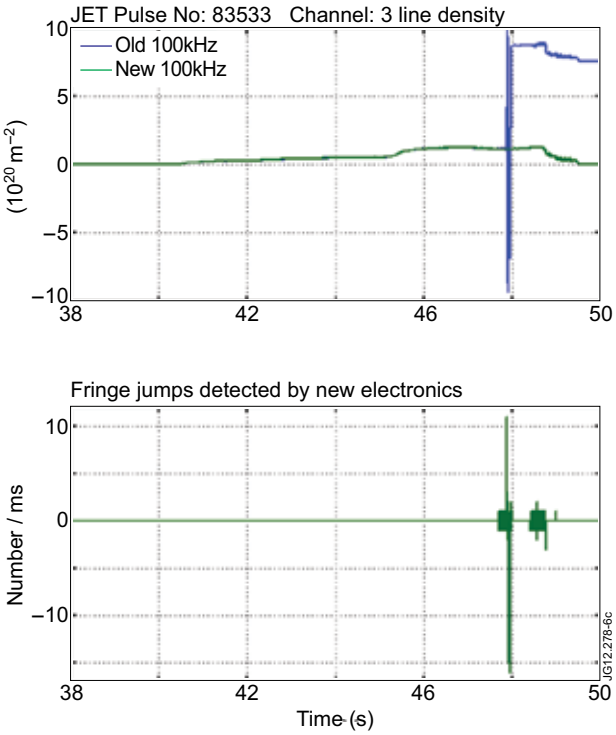

Figure 6: Top Comparison of the measured line density, bottom: detected fringe jumps per millisecond.

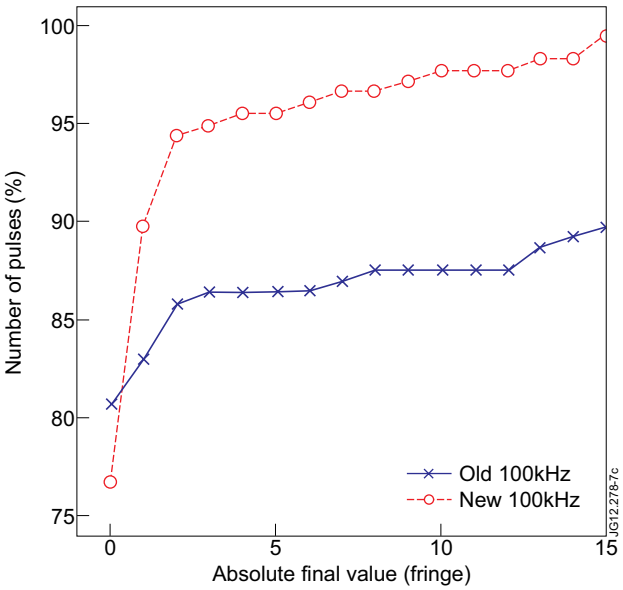

Figure 7: Statistics on 177 disruption-free pulses with simultaneous data on channel 3 from JET Pulse No's: 83225 to 83646.